HAL
open science

Age stability of La(Fe,Si)13 hydrides with giant magnetocaloric effects

He Zhou, Yi Long, Salvatore Miraglia, Florence Porcher, Hu Zhang

To cite this version:

He Zhou, Yi Long, Salvatore Miraglia, Florence Porcher, Hu Zhang. Age stability of La(Fe,Si)13 hydrides with giant magnetocaloric effects. Rare Metals, 2021, 41, pp.992-1001. 10.1007/s12598-021-01849-3 . hal-03447163

HAL Id: hal-03447163

https://hal.science/hal-03447163

Submitted on 7 Dec 2021

HAL is a multi-disciplinary open access archive for the deposit and dissemination of scientific research documents, whether they are published or not. The documents may come from teaching and research institutions in France or abroad, or from public or private research centers.

L'archive ouverte pluridisciplinaire **HAL**, est destinée au dépôt et à la diffusion de documents scientifiques de niveau recherche, publiés ou non, émanant des établissements d'enseignement et de recherche français ou étrangers, des laboratoires publics ou privés.

Study on the age stability of $La(Fe,Si)_{13}$ hydrides with giant magnetocaloric effects

He Zhou [a], Yi Long [a], Salvatore Miraglia [b], Florence Porcher [c] Hu Zhang [a,*]

[a] *School of Materials Science and Engineering, University of Science and Technology Beijing, Beijing 100083, People's Republic of China.*

[b] *Université Grenoble Alpes, CNRS, Institut Néel, 25 Rue des Martyrs, 38042 Grenoble, France.*

[c] *Laboratoire Leon Brillouin, UMR12 CEA-CNRS, Bat. 563 CEA Saclay, F-91191 Gif sur Yvette Cedex, France.*

Abstract

The Curie temperatures (T_C) of fully hydrogenated $La_{0.7}Ce_{0.3}Fe_{13-x-y}Mn_xSi_y$ compounds are raised to near room temperature. The age stability of $La_{0.7}Ce_{0.3}Fe_{11.5-x}Mn_xSi_{1.5}$ hydrides held at room temperature was investigated. This result indicates that the H content will slowly decrease in the hydrides, leading to a decrease of T_C. However, the T_C decreases slightly and no age splitting occurs after the hydrides are held at room temperature for two years, indicating the excellent age stability of fully hydrogenated $La(Fe,Si)_{13}$-based compounds. Further structural analysis by neutron diffraction shows that the Mn atoms preferentially substitute Fe in the 96i sites. The T_C of $La_{0.7}Ce_{0.3}Fe_{11.55-y}Mn_ySi_{1.45}$ hydrides can be adjusted to the desired working temperature by regulating the Mn content based on the linear relationship between T_C and Mn content. Moreover, the $La_{0.7}Ce_{0.3}Fe_{11.55-y}Mn_ySi_{1.45}$ hydrides exhibit a giant magnetic entropy change of 15 J/kg K under a low magnetic

* Corresponding author at: School of Materials Science and Engineering, University of Science and Technology Beijing, Beijing, 100083, China. Tel.: +86-10-62334807.

E-mail address: zhanghu@ustb.edu.cn

field change of 0−1 T. As a result, the giant magnetocaloric effect, linearly adjustable T_C and excellent age stability make the $La_{0.7}Ce_{0.3}Fe_{11.55-y}Mn_ySi_{1.45}$ hydrides one of the ideal candidates for room temperature magnetic refrigerants.

Keywords: Magnetocaloric effect; $La(Fe,Si)_{13}$; Hydrides; Stability

1. Introduction

The $La(Fe,Si)_{13}$ compounds with cubic $NaZn_{13}$-type structure (1:13 phase) have been concerned as promising magnetic refrigeration materials owing to the advantages of giant magnetocaloric effect (MCE), tunable Curie temperature (T_C), non-toxicity and low cost [1-3]. However, the T_C of $La(Fe,Si)_{13}$ compounds is lower than 210 K [4], which cannot meet the requirements of room-temperature magnetic refrigeration. Introducing interstitial H atoms into $La(Fe,Si)_{13}$ compounds is considered as the most efficient way to improve the T_C and keep the large MCE. For $La(Fe_{0.88}Si_{0.12})_{13}H_y$ compounds, the T_C increases from 195 K to 330 K when y varies from 0 to 1.5, and the giant MCE is retained [5]. Therefore, the T_C can be adjusted to the desired working temperature by precisely regulating the H content, which can be realized by controlling the hydrogen absorption or desorption process parameters, such as hydrogen gas pressure, treatment temperature and hydrogenation time [6]. Nevertheless, it is very difficult to precisely adjust the T_C by regulating the H content because the T_C of $La(Fe,Si)_{13}$ compounds is very sensitive to H content. Moreover, the partially hydrogenated $La(Fe,Si)_{13}$ compounds cannot guarantee the long-term stability when they are held near their T_Cs [7, 8]. Therefore, in order to adjust the T_C to near room temperature, it is a suitable way to adjust the T_C of parent compounds by composition regulation and then absorb hydrogen to saturation.

For $La(Fe,Si)_{13}$ compounds, rare earths substitution to La or transition metals to Fe can adjust the T_C. Modest substitution of Co, Ni, Mn or Cr for Fe would not alter the $NaZn_{13}$-type crystal structure of $La(Fe,Si)_{13}$ compounds [9-13]. Previous studies

have revealed that Co or Ni atoms occupy 96*i* sites [10, 14] and Cr atoms occupy 8*b* sites [12] in $La(Fe,Si)_{13}$ compounds, while no related work has been devoted to analyze the Mn location. Both the substitution of Ce for La and the substitution of Mn for Fe can remarkably decrease the T_C of $La(Fe,Si)_{13}$ compounds. The addition of Ce can strengthen the first-order magnetic transition and enhance the magnetic entropy change [15]. Nevertheless, the nature of magnetic transition varies from first-order to second-order and the magnetic entropy change gradually decreases with the increase of Mn content [11, 16]. $La_{1-z}Ce_z(Fe_{x-y}Mn_ySi_{1-x})_{13}$ compounds can still keep the itinerant-electron metamagnetic transition and exhibit strong magnetocaloric effect in a broad temperature range from 19 to 180 K [17]. The T_C of the fully hydrogenated $La_{1-z}Ce_z(Fe_{x-y}Mn_ySi_{1-x})_{13}$ compounds can be raised to near room temperature, and the hydrides show large magnetic entropy changes [18-21]. As a result, $La_{1-z}Ce_z(Fe_{x-y}Mn_ySi_{1-x})_{13}$ hydrides are ideal room temperature magnetic refrigerants. However, for the hydrides, the premise of application is to ensure the long-term stability when they are used at temperatures close to their T_Cs. Unfortunately, few works have been reported on the age stability of fully hydrogenated $La(Fe,Si)_{13}$ compounds.

In present work, the fully hydrogenated $La_{0.7}Ce_{0.3}Fe_{11.5-x}Mn_xSi_{1.5}$ compounds exhibit excellent age stability. For $La_{0.7}Ce_{0.3}Fe_{11.55-y}Mn_ySi_{1.45}$ hydrides, a giant magnetic entropy change of 15 J/kg K under a low magnetic field change of 0−1 T is obtained, and the T_C can be regulated precisely based on the linear relationship between T_C and Mn content. Moreover, the crystallographic structure and Mn location

of $La_{0.7}Ce_{0.3}Fe_{11.28}Mn_{0.22}Si_{1.5}$ hydride were analyzed by neutron powder diffraction.

2. Experimental

$La_{0.7}Ce_{0.3}Fe_{11.5-x}Mn_xSi_{1.5}$ (x = 0.125, 0.20, 0.22, 0.26) and $La_{0.7}Ce_{0.3}Fe_{11.55-y}Mn_ySi_{1.45}$ (y = 0.175, 0.19, 0.22, 0.235) ingots were prepared by induction melting. The purity of the raw materials is at least 99.9 wt.%. Then the ingots were processed into ribbons by melt-spinning method. The ribbons were sealed in a quartz tube with an argon atmosphere and annealed at 1393 K for 20 hours followed by ice-water quenching. The structure of the ribbons was identified by X-ray powder diffraction (XRD) using Cu $K\alpha$ radiation at room temperature. The phase compositions of the ribbons were observed by scanning electron microscopy (SEM). The ribbons were broken and ground into powders with size less than 150 μm, and then annealed in a hydrogen atmosphere of 0.2 MPa at 623 K for 5 days. The hydrogen concentrations of these hydrides were determined by the hot-extraction method. High-resolution steady state neutron diffraction patterns have been recorded at room temperature on the 3T2 diffractometer of Laboratoire Léon Brillouin with an incident neutron wavelength of 1.225 Å. The neutron diffraction patterns collected over the range 2θ = 5−120° with a step increment of 0.05° were analyzed by Rietveld refinement via the GSAS/EXPGUI software [22]. The different scanning calorimetry (DSC) measurements were carried out using DSC 6220 with a heating/cooling rate of 10 K/min. Magnetization was measured using a cryogen-free cryocooler-based physical property measurement system (model VersaLab) from Quantum Design Inc.

3. Results and discussion

Figure 1(a) shows the powder XRD patterns of $La_{0.7}Ce_{0.3}Fe_{11.55-y}Mn_ySi_{1.45}$ (y = 0.175, 0.19, 0.22, 0.235) compounds at room temperature. It reveals that all ribbons annealed at 1393 K for 20 hours are composed of the $NaZn_{13}$-type phase and no α-Fe phase is present in the XRD patterns. In addition, further microstructure analysis shows that the phase composition of the ribbons is mainly 1:13 phase, accompanied by a very small amount of La-rich phase, as shown in the inset of Fig. 1(a), which corresponds to the backscattered SEM micrograph of y = 0.235 compound. The amount of La-rich phase is too small to be detected in the XRD patterns.

The Neutron diffraction experiments were performed on $La_{0.7}Ce_{0.3}Fe_{11.28}Mn_{0.22}Si_{1.5}$ hydride at 300 K (T_C = 270 K) to get the knowledge of Mn location in Mn doped $La(Fe,Si)_{13}$ compounds. Figure 1(b) shows the observed and calculated neutron diffraction patterns for $La_{0.7}Ce_{0.3}Fe_{11.28}Mn_{0.22}Si_{1.5}$ hydride. It can be seen that the hydride crystallizes in the $NaZn_{13}$-type structure with a small amount of α-Fe phase (~4.6 wt%) as a secondary phase. The schematic structure of the 1/8 part of a cubic unit cell for $La(Fe,Si)_{13}$-based compounds is displayed in Fig. 1(b). The rare earth La atoms are located in site 8*a* (1/4, 1/4, 1/4). Fe atoms are located in two different symmetry sites, Fe Ⅰ at 8*b* (0, 0, 0) and Fe Ⅱ at 96*i* (0, *y*, *z*) [23]. Si atoms preferentially substitute Fe in the 96*i* site [24]. The interstitial H atoms occupy the 24*d* interstitial sites [25]. Based on the above atom positions, the result of Rietveld refinement shows that the Mn atoms locate at the 96*i* site of Fe Ⅱ, not at the 8*b* site. Moreover, the refined Mn site occupancies are about 0.17 (2) on the 96*i* sites, which is less than the starting nominal composition due to the α-(Fe,Mn/Si) secondary phase

and the weight loss during the induction melting process.

The T_C of $La_{0.7}Ce_{0.3}Fe_{11.5-x}Mn_xSi_{1.5}$ hydrides and $La_{0.7}Ce_{0.3}Fe_{11.55-y}Mn_ySi_{1.45}$ hydrides can be obtained by the DSC measurements. The T_C is defined as the temperature corresponding to the peak of the DSC curve, and the test sample is randomly selected from the powder. In order to prove the homogeneity of the hydrogenated powders, the T_C was measured by using different samples randomly selected from the powders. Figure 2 shows DSC heat flow curves during heating for three samples randomly selected from the powders of (a) $La_{0.7}Ce_{0.3}Fe_{11.28}Mn_{0.22}Si_{1.5}$ hydride and (b) $La_{0.7}Ce_{0.3}Fe_{11.33}Mn_{0.22}Si_{1.45}$ hydride, other hydrides are not shown in the figure because they display similar results. It can be seen that the three samples of each hydride exhibit the identical endothermic peaks and the T_C exhibits a small fluctuation of less than 0.5 K, which implies the homogeneous distribution of H atoms in these hydrides. The DSC curves during heating for $La_{0.7}Ce_{0.3}Fe_{11.5-x}Mn_xSi_{1.5}$ and $La_{0.7}Ce_{0.3}Fe_{11.55-y}Mn_ySi_{1.45}$ hydrides are shown in Fig. 2(c) and (d), respectively. The T_Cs of these hydrides are raised to near room temperature. Moreover, the T_C gradually decreases with increasing Mn content. This result confirms that it is an effective method to adjust the T_C of hydrides by regulating the composition of parent compounds.

As mentioned above, the partially hydrogenated $La(Fe,Si)_{13}$-based compounds are unstable. The transition would split into two separate transitions with different transition temperatures when the hydrides are held close to their T_C due to the hydrogen diffusion between paramagnetic and ferromagnetic phases [7, 21]. The age

splitting phenomenon is a significant detriment to the magnetic refrigeration performance. Nevertheless, the full hydrogenation can inhibit the age splitting phenomenon, and the fully hydrogenated $La(Fe,Si)_{13}$-based compounds show an improved stability [8]. The hydrogenated $La_{0.7}Ce_{0.3}Fe_{11.5-x}Mn_xSi_{1.5}$ and $La_{0.7}Ce_{0.3}Fe_{11.55-y}Mn_ySi_{1.45}$ compounds are stored at room temperature (285−300 K), which is close to their T_C. Figure 2(e) displays the DSC curve of x = 0.125 hydride held at room temperature for one year, and other hydrides have similar results. It can be seen that the hydrides still exhibit a single sharp transition peak and no age splitting appears. This result proves that these compounds are fully hydrogenated. The x = 0.125 hydride was thermally cycled around the T_C on DSC to further investigate the functional fatigue behavior. Figure 2(e) shows the DSC curves of x = 0.125 hydride at the selected transition cycles. During 100 cycles in this study, it can be observed that the transition calorimetric profiles remain almost unchanged. The peak positions and peak heights manifest trivial change, as shown in the magnified figure of a selected region in Fig. 2(e). As a result, the $La(Fe,Si)_{13}$-based hydrides possess robust functional stability.

In order to study the age stability of hydrides, the T_Cs of $La_{0.7}Ce_{0.3}Fe_{11.5-x}Mn_xSi_{1.5}$ hydrides stored for different time were measured. The T_C measurement of each sample was repeated for three times, and the T_C is defined as the average of three measurement results. Figure 3(a) shows the T_C of the $La_{0.7}Ce_{0.3}Fe_{11.5-x}Mn_xSi_{1.5}$ hydrides measured after initial preparation, after one year, and after two years when held at room temperature. The T_C decreases gradually when

the hydrides were held at room temperature for a longer time. Moreover, the T_C of the hydrides held at room temperature for two years exhibits a more significant decrease than that of the hydrides held for one year. The T_C of $La(Fe,Si)_{13}$ compounds is very sensitive to H content, and a slight variation of H content will lead to the significant change of T_C. Therefore, the decrease of T_C may be related to the reduction of H content for $La_{0.7}Ce_{0.3}Fe_{11.5-x}Mn_xSi_{1.5}$ hydrides due to the instability of H atoms in $La(Fe,Si)_{13}$-based compounds. It can be found from Fig. 3(a) that the T_C of x = 0.125 compound is in the room temperature range, the reduction of H content most likely results from the magnetovolume effect of $La(Fe,Si)_{13}$ compounds. The repeated expansion/shrinkage of cell volume will drive H atoms away from the interstitial positions when the hydrides are kept near their T_C for a long time, resulting in the reduction of H content and the decrease of T_C. At the same time, it can be seen that the T_C of x = 0.20, 0.22 and 0.26 hydrides is slightly lower than the room temperature, but these hydrides would still undergo partial phase transition because the T_C is very close to the storage temperature. In addition, it is noteworthy that the DSC curves do not show age splitting for the hydrides held at room temperature for two years, implying the long-term stability of the hydrides. The difference in Curie temperature (ΔT_C) between the initially-prepared samples and the samples held at room temperature for two years is shown in Fig. 3(a). It can be observed that a slight decrease of about 5.5 K in T_C for the hydrides held at room temperature for two years, suggesting the excellent age stability of fully hydrogenated $La(Fe,Si)_{13}$-based compounds. Moreover, the slight variation of ΔT_C with the change of Mn content

indicates that Mn content does not have much effect on the age stability of $La_{0.7}Ce_{0.3}Fe_{11.5-x}Mn_xSi_{1.5}$ hydrides.

Figure 3(b) shows the latent heat as a function of Mn content for $La_{0.7}Ce_{0.3}Fe_{11.5-x}Mn_xSi_{1.5}$ hydrides held at room temperature for different time. The latent heat during heating can be calculated by integrating the area of DSC endothermic peak, as shown in the inset of Fig. 3(b). For $La_{0.7}Ce_{0.3}Fe_{11.5-x}Mn_xSi_{1.5}$ hydrides, the latent heat gradually increases as the hydrides are held at room temperature for a longer time. The increase of latent heat demonstrates the enhancement of first-order magnetic transition. In $La(Fe,Si)_{13}$ compounds, the hydrogenation will weaken the itinerant-electron metamagnetic transition and the first-order magnetic transition [26], that is, more H content will decrease the latent heat. As a result, the increase of latent heat further confirms the H content will slowly decrease when the hydrides are held at room temperature.

The magnetization isotherms of the x = 0.22 and y = 0.22 hydrides for the magnetization and demagnetization processes are shown in Fig. 4(a) and (b), respectively. The maximal hysteresis loss (enclosed area in a field cycle) under a magnetic field change of 0−3 T is 1.2 J/kg for x = 0.22 hydride and 5.1 J/kg for y = 0.22 hydride. This result indicates that the first-order nature of field-induced itinerant electron metamagnetic transition is strengthened when the Si content decreases from 1.5 to 1.45. However, the hysteresis loss of y = 0.22 hydride is still much lower than those of many other magnetocaloric materials experiencing first-order phase transitions; this is highly desirable for the improvement of the effective magnetic

refrigerant capacity.

The Arrott plot is applied to further study the nature of magnetic transition. The Arrott plot of first-order magnetic transition exhibits negative slope or inflection point, while the slope is positive for second-order magnetic transition. The Arrott plots of $La_{0.7}Ce_{0.3}Fe_{11.5-x}Mn_xSi_{1.5}$ and $La_{0.7}Ce_{0.3}Fe_{11.55-y}Mn_ySi_{1.45}$ hydrides near their T_C are shown in Fig. 4(c) and (d), respectively. It can be found that these hydrides except x = 0.26 hydride show obviously negative slope, indicating that the saturated hydrogenated $La_{0.7}Ce_{0.3}Fe_{11.5-x}Mn_xSi_{1.5}$ and $La_{0.7}Ce_{0.3}Fe_{11.55-y}Mn_ySi_{1.45}$ compounds still retain the characteristic of first-order magnetic transition. Moreover, for $La_{0.7}Ce_{0.3}Fe_{11.5-x}Mn_xSi_{1.5}$ hydrides, the negative slope gradually decreases with increasing Mn content, indicating that the substitution of Mn for Fe would weaken the first-order magnetic transition. The x = 0.26 hydride exhibits a clearly positive slope, implying that the nature of magnetic transition changes from first-order to second-order. However, as shown in the inset of Fig. 4(c), the large endothermic and exothermic DSC peaks observed during heating and cooling and the distinct thermal hysteresis reveal that the x = 0.26 hydride experience a first-order magnetic transition. Herein, a recently reported quantitative criterion [27] is used to further determine the order of magnetic phase transition. The field dependence of the magnetic entropy change (ΔS_M) can be expressed as:

$$\Delta S_M \propto H^n \tag{1}$$

where the ΔS_M can be calculated from the isothermal magnetization curves by using the Maxwell relation [28]:

$$\Delta S_M(T,H) = \mu_0 \int_0^H \left(\frac{\partial M}{\partial T}\right)_H dH \tag{2}$$

The exponent n can be calculated using [27]

$$n(T,H) = \frac{\mathrm{d}\ln|\Delta S_M|}{\mathrm{d}\ln H} \tag{3}$$

The exponent n presents a maximum of $n > 2$ only for first-order magnetic phase transition. Therefore, the existence of this overshoot of n above 2 is the criterion to determine a first-order magnetic transition [27]. The temperature dependence of the exponent n under a maximum field of 2 T for $x = 0.26$ hydride is shown in Fig. 4(e). It can be seen that the n value tends to 1 at the temperature below the T_C and n value tends to 2 at the temperature above the T_C, which is consistent with previous reports [27]. Moreover, the minimum of n is followed by a maximum with a value larger than 2. The existence of $n > 2$ is the distinctive feature of first-order magnetic transition. As a result, this result confirms that the $x = 0.26$ hydride undergoes a weak first-order magnetic transition.

The T_C as a function of Mn content for $La_{0.7}Ce_{0.3}Fe_{11.55-y}Mn_ySi_{1.45}$ compounds and their hydrides are displayed in Fig. 5(a). For $La_{0.7}Ce_{0.3}Fe_{11.55-y}Mn_ySi_{1.45}$ compounds, the T_C can obviously be raised to near room temperature after hydrogenation, and the T_C of hydrides gradually decreases with the increase of Mn content, which is consistent with parent samples. Moreover, the linear relationship between T_C and Mn content implies that the T_C of hydrides can be adjusted to the desired working temperature by regulating the Mn content. The H content δ in $La_{0.7}Ce_{0.3}Fe_{11.55-y}Mn_ySi_{1.45}H_\delta$ compounds is determined to be about 1.8, which

remains constant for different Mn contents, implying that the Mn content will not have a significant effect on the H content of fully hydrogenated $La(Fe,Si)_{13}$ compounds. Figure 5(b) displays the lattice constant as a function of Mn content for $La_{0.7}Ce_{0.3}Fe_{11.55-y}Mn_ySi_{1.45}$ compounds and their hydrides. It can be clearly observed that the lattice constant increases significantly after hydrogenation, indicating that the introduction of interstitial H atoms will cause lattice expansion. For $La(Fe,Si)_{13}$ compounds, the T_C is mainly determined by the Fe-Fe interactions [26, 29]. Similarly, the average Fe-Fe distance also increases after hydrogenation, as shown in Fig. 5(b). The larger Fe-Fe distance would strengthen the exchange interaction between Fe-Fe atoms by decreasing the overlap of Fe 3*d* wave functions, resulting in the increase of T_C [26]. Nevertheless, it can be found that the Fe-Fe distance gradually decreases with increasing Mn content for $La_{0.7}Ce_{0.3}Fe_{11.55-y}Mn_ySi_{1.45}$ compounds and their hydrides. The substitution of Mn with larger size for Fe at 96*i* sites would squeeze the surrounding Fe atoms, which may lead to the reduction of Fe-Fe distance. The shorter Fe-Fe distance would weaken the exchange interaction between Fe-Fe atoms and decrease T_C. Moreover, it is worthwhile to note that the rate of T_C change of hydrogenated samples with Mn content is lower than that of the parent samples (Fig. 5(a)), which implies that hydrogenation will weaken the effect of Mn atoms on the T_C. The lattice expansion caused by interstitial H atoms may weaken the squeezing of Mn atoms on the surrounding Fe atoms, thus weakening the effect of Mn atoms on T_C after hydrogenation. Unfortunately, the Rietveld analysis cannot prove this speculation due to the slight variation of Mn content.

Figure 6 shows the temperature dependence of $-\Delta S_M$ for $La_{0.7}Ce_{0.3}Fe_{11.5-x}Mn_xSi_{1.5}$ and $La_{0.7}Ce_{0.3}Fe_{11.55-y}Mn_ySi_{1.45}$ hydrides under a magnetic field change of 1 T. It can be seen that the magnetic entropy change gradually decreases with increasing Mn content due to the weakening of the first-order magnetic transition for $La_{0.7}Ce_{0.3}Fe_{11.5-x}Mn_xSi_{1.5}$ hydrides. Nevertheless, unlike $La_{0.7}Ce_{0.3}Fe_{11.5-x}Mn_xSi_{1.5}$ hydrides, the ΔS_M $La_{0.7}Ce_{0.3}Fe_{11.55-y}Mn_ySi_{1.45}$ hydrides does not show a drastic change with the variation of Mn content. The inset of Fig. 6 plots the maximum $-\Delta S_M$ value as a function of Mn content. The magnetic entropy changes of $La_{0.7}Ce_{0.3}Fe_{11.55-y}Mn_ySi_{1.45}$ hydrides are remarkably larger than those of $La_{0.7}Ce_{0.3}Fe_{11.5-x}Mn_xSi_{1.5}$ hydrides. The $La_{0.7}Ce_{0.3}Fe_{11.55-y}Mn_ySi_{1.45}$ hydrides exhibit a giant $-\Delta S_M$ of ~15 J/kg K under a low field change of 0−1 T, which is larger than those of many typical room temperature magnetocaloric materials, such as Gd (5.2 J/kg K, 0−2 T) [30], $Gd_5Si_2Ge_2$ (14 J/kg K, 0−2 T) [30], $MnFe_{0.95}P_{0.595}B_{0.075}Si_{0.33}$ (9.8 J/kg K, 0−1 T) [31], and $Mn_{0.5}Fe_{0.5}NiSi_{0.945}Al_{0.055}$ (9.5 J/kg K, 0−1 T) [32]. As a result, the $La_{0.7}Ce_{0.3}Fe_{11.55-y}Mn_ySi_{1.45}$ hydrides with giant MCE, linearly adjustable T_C and excellent age stability are one of the most practical candidates for room temperature magnetic refrigerants.

4. Conclusions

The crystallographic structure of $La_{0.7}Ce_{0.3}Fe_{11.28}Mn_{0.22}Si_{1.5}$ hydride was investigated by neutron powder diffraction. The result indicates the Mn atoms preferentially substitute Fe in the 96*i* sites. The T_C of fully hydrogenated $La_{0.7}Ce_{0.3}Fe_{13-x-y}Mn_xSi_y$ compounds are raised to near room temperature. The age

stability study shows that the T_C of the $La_{0.7}Ce_{0.3}Fe_{11.5-x}Mn_xSi_{1.5}$ hydrides held at room temperature gradually decrease due to the slow reduction of H content in the hydrides. The T_C decreases slightly and no age splitting occurs for $La_{0.7}Ce_{0.3}Fe_{11.5-x}Mn_xSi_{1.5}$ hydrides held at room temperature for two years, suggesting the excellent age stability of fully hydrogenated $La(Fe,Si)_{13}$-based compounds. The fully hydrogenated $La_{0.7}Ce_{0.3}Fe_{11.5-x}Mn_xSi_{1.5}$ and $La_{0.7}Ce_{0.3}Fe_{11.55-y}Mn_ySi_{1.45}$ compounds maintain the first-order magnetic transition. The $La_{0.7}Ce_{0.3}Fe_{11.55-y}Mn_ySi_{1.45}$ hydrides exhibit a giant magnetic entropy change of 15 J/kg K under a low magnetic field change of 0−1 T. Moreover, the T_C of hydrides can be adjusted to the desired working temperature by regulating the Mn content of parent samples. All of these results demonstrate $La_{0.7}Ce_{0.3}Fe_{11.55-y}Mn_ySi_{1.45}$ hydrides are desirable room temperature magnetic refrigerants.

References

[1] B.G. Shen, J.R. Sun, F.X. Hu, H.W. Zhang, Z.H. Cheng, Recent progress in exploring magnetocaloric materials, Adv. Mater. 21 (2009) 4545-4564.

[2] V. Franco, J.S. Blázquez, B. Ingale, A. Conde, The magnetocaloric effect and magnetic refrigeration near room temperature: materials and models, Annu. Rev. Mater. Res. 42 (2012) 305-342.

[3] H. Zhang, F.X. Hu, J.R. Sun, B.G. Shen, Effects of interstitial H and/or C atoms on the magnetic and magnetocaloric properties of La(Fe, Si)$_{13}$-based compounds, Sci. China-Phys. Mech. Astron. 56 (2013) 2302-2311.

[4] Y.F. Chen, F. Wang, B.G. Shen, J.R. Sun, G.J. Wang, F.X. Hu, Z.H. Cheng, T. Zhu, Effects of carbon on magnetic properties and magnetic entropy change of the $LaFe_{11.5}Si_{1.5}$ compound, J. Appl. Phys. 93 (2003) 6981-6983.

[5] A. Fujita, S. Fujieda, Y. Hasegawa, K. Fukamichi, Itinerant-electron metamagnetic transition and large magnetocaloric effects in $La(Fe_xSi_{1-x})_{13}$ compounds and their hydrides, Phys. Rev. B 67 (2003) 104416.

[6] J.W. Wang, Y.G. Chen, Y.B. Tang, S.F. Xiao, T. Liu, E.Y. Zhang, The hydrogenation behavior of $LaFe_{11.44}Si_{1.56}$ magnetic refrigerating alloy, J. Alloys Compd. 485 (2009) 313-315.

[7] C.B. Zimm, S.A. Jacobs, Age splitting of the $La(Fe_{1-x}Si_x)_{13}H_y$ first order magnetocaloric transition and its thermal restoration, J. Appl. Phys. 113 (2013) 17A908.

[8] A. Barcza, M. Katter, V. Zellmann, S. Russek, S. Jacobs, C. Zimm, Stability and

magnetocaloric properties of sintered $La(Fe,Mn,Si)_{13}H_z$ alloys, IEEE Trans. Magn. 47 (2011) 3391-3394.

[9] M. Balli, D. Fruchart, D. Gignoux, Optimization of $La(Fe,Co)_{13-x}Si_x$ based compounds for magnetic refrigeration, J. Phys.: Condens. Matter 19 (2007) 236230.

[10] L.M. Moreno-Ramírez, C. Romero-Muñiz, J.Y. Law, V. Franco, A. Conde, I.A. Radulov, F. Maccari, K.P. Skokov, O. Gutfleisch, The role of Ni in modifying the order of the phase transition of $La(Fe,Ni,Si)_{13}$, Acta Mater. 160 (2018) 137-146.

[11] M. Krautz, K. Skokov, T. Gottschall, C.S. Teixeira, A. Waske, J. Liu, L. Schultz, O. Gutfleisch, Systematic investigation of Mn substituted $La(Fe,Si)_{13}$ alloys and their hydrides for room-temperature magnetocaloric application, J. Alloys Compd. 598 (2014) 27-32.

[12] L.M. Moreno-Ramírez, C. Romero-Muñiz, J.Y. Law, V. Franco, A. Conde, I.A. Radulov, F. Maccari, K.P. Skokov, O. Gutfleisch, Tunable first order transition in $La(Fe,Cr,Si)_{13}$ compounds: Retaining magnetocaloric response despite a magnetic moment reduction, Acta Mater. 175 (2019) 406-414.

[13] S.T. Zong, Y. Long, The influence of Cr and Ni on the character of magnetic phase transition in $LaFe_{11.52-x}M_xSi_{1.48}$ alloys, AIP Adv. 8 (2018) 048101.

[14] F.W. Wang, A. Kurbakov, G.J. Wang, F.X. Hu, B.G. Shen, Z.H. Cheng, Strong interplay between structure and magnetism in $LaFe_{11.3}Co_{0.6}Si_{1.1}$: A neutron diffraction study, Physica B 385-386 (2006) 343-345.

[15] S. Fujieda, A. Fujita, K. Fukamichi, N. Hirano, S. Nagaya, Large magnetocaloric effects enhanced by partial substitution of Ce for La in $La(Fe_{0.88}Si_{0.12})_{13}$ compound, J.

Alloys Compd. 408-412 (2006) 1165-1168.

[16] F. Wang, Y.F. Chen, G.J. Wang, B.G. Shen, The effect of Mn substitution in $LaFe_{11.7}Si_{1.3}$ compound on the magnetic properties and magnetic entropy changes, J. Phys. D: Appl. Phys. 36 (2003) 1-3.

[17] S. Fujieda, A. Fujita, N. Kawamoto, K. Fukamichi, Strong magnetocaloric effects in $La_{1-z}Ce_z(Fe_{x-y}Mn_ySi_{1-x})_{13}$ at low temperatures, Appl. Phys. Lett. 89 (2006) 062504.

[18] C.L. Wang, Y. Long, T. Ma, B. Fu, R.C. Ye, Y.Q. Chang, F.X. Hu, J. Shen, The hydrogen absorption properties and magnetocaloric effect of $La_{0.8}Ce_{0.2}(Fe_{1-x}Mn_x)_{11.5}Si_{1.5}H_y$, J. Appl. Phys. 109 (2011) 07A910.

[19] W. Xia, J.H. Huang, N.K. Sun, C.L. Lui, Z.Q. Ou, L. Song, Influence of powder bonding on mechanical properties and magnetocaloric effects of $La_{0.9}Ce_{0.1}(Fe,Mn)_{11.7}Si_{1.3}H_{1.8}$, J. Alloys Compd. 635 (2015) 124-128.

[20] Y.X. Wang, H. Zhang, E.K. Liu, X.C. Zhong, K. Tao, M.L. Wu, C.F. Xing, Y.N. Xiao, J. Liu, Y. Long, Outstanding comprehensive performance of $La(Fe, Si)_{13}H_y$/In composite with durable service life for magnetic refrigeration, Adv. Electron. Mater. 4 (2018) 1700636.

[21] A. Fujita, Influence of electronic and metallographic structures on hydrogen redistribution in $La(Fe,Si)_{13}$-based magnetocaloric compounds, Acta Mater. 169 (2019) 162-171.

[22] B.H. Toby, EXPGUI, a graphical user interface for GSAS, J. Appl. Crystallogr. 34 (2001) 210-213.

[23] M. Rosca, M. Balli, D. Fruchart, D. Gignoux, E.K. Hlil, S. Miraglia, B.

Ouladdiaf, P. Wolfers, Neutron diffraction study of $LaFe_{11.31}Si_{1.69}$ and $LaFe_{11.31}Si_{1.69}H_{1.45}$ compounds, J. Alloys Compd. 490 (2010) 50-55.

[24] J. Lyubina, Recent advances in the microstructure design of materials for near room temperature magnetic cooling (invited), J. Appl. Phys. 109 (2011) 07A902.

[25] S. Fujieda, A. Fujita, K. Fukamichi, Y. Yamaguchi, K. Ohoyama, Neutron diffraction and isotropic volume expansion caused by deuterium absorption into $La(Fe_{0.88}Si_{0.12})_{13}$, J. Phys. Soc. Jpn. 77 (2011) 074722.

[26] J.L. Zhao, J. Shen, F.X. Hu, Y.X. Li, J.R. Sun, B.G. Shen, Reduction of magnetic hysteresis loss in $La_{0.5}Pr_{0.5}Fe_{11.4}Si_{1.6}H_x$ hydrides with large magnetocaloric effects, J. Appl. Phys. 107 (2010) 113911.

[27] J.Y. Law, V. Franco, L.M. Moreno-Ramírez, A. Conde, D.Y. Karpenkov, I. Radulov, K.P. Skokov, O. Gutfleisch, A quantitative criterion for determining the order of magnetic phase transitions using the magnetocaloric effect, Nat. Commun. 9 (2018) 2680.

[28] K.A. Gschneidner Jr., V.K. Pecharsky, A.O. Tsokol, Recent developments in magnetocaloric materials, Rep. Prog. Phys. 68 (2005) 1479-1539.

[29] W. Li, R.J. Huang, W. Wang, H.M. Liu, Y.M. Han, C.J. Huang, L.F. Li, Low-temperature negative thermal expansion property of Mn doped $La(Fe,Si)_{13}$ compounds, J. Alloys Compd. 628 (2015) 308-310.

[30] V.K. Pecharsky, K.A. Gschneidner Jr., Giant Magnetocaloric Effect in $Gd_5(Si_2Ge_2)$, Phys. Rev. Lett. 78 (1997) 4494-4497.

[31] F. Guillou, G. Porcari, H. Yibole, N. van Dijk, E. Brück, Taming the first-order

transition in giant magnetocaloric materials, Adv. Mater. 26 (2014) 2671-2675.

[32] A. Biswas, A.K. Pathak, N.A. Zarkevich, X.B. Liu, Y. Mudryk, V. Balema, D.D. Johnson, V.K. Pecharsky, Designed materials with the giant magnetocaloric effect near room temperature, Acta Mater. 180 (2019) 341-348.

Figure captions

Fig. 1. (a) The powder XRD patterns of $La_{0.7}Ce_{0.3}Fe_{11.55-y}Mn_ySi_{1.45}$ (y = 0.175, 0.19, 0.22, 0.235) compounds at room temperature. The inset shows the backscattered SEM micrograph of y = 0.235 compound. (b) Neutron powder diffraction patterns of $La_{0.7}Ce_{0.3}Fe_{11.28}Mn_{0.22}Si_{1.5}$ hydride at 300 K. (c) Schematic structure of the 1/8 part of a cubic unit cell for $La(Fe,Si)_{13}$-based compounds.

Fig. 2. DSC curves of three samples for (a) $La_{0.7}Ce_{0.3}Fe_{11.28}Mn_{0.22}Si_{1.5}$ hydride and (b) $La_{0.7}Ce_{0.3}Fe_{11.33}Mn_{0.22}Si_{1.45}$ hydride. The DSC curves during heating for (c) $La_{0.7}Ce_{0.3}Fe_{11.5-x}Mn_xSi_{1.5}$ hydrides and (d) $La_{0.7}Ce_{0.3}Fe_{11.55-y}Mn_ySi_{1.45}$ hydrides. (e) DSC curves of x = 0.125 hydride at the selected transition cycles.

Fig. 3. (a) The T_C of the $La_{0.7}Ce_{0.3}Fe_{11.5-x}Mn_xSi_{1.5}$ hydrides measured after initial preparation, after one year, and after two years when held at room temperature and the ΔT_C between the initially-prepared samples and the samples held at room temperature for two years for $La_{0.7}Ce_{0.3}Fe_{11.5-x}Mn_xSi_{1.5}$ hydrides. (b) The latent heat as a function of Mn content for $La_{0.7}Ce_{0.3}Fe_{11.5-x}Mn_xSi_{1.5}$ hydrides held at room temperature for different time. The inset shows the schematic illustration of latent heat calculation.

Fig. 4. Magnetization isotherms with magnetizing and demagnetizing processes for (a) x = 0.22 hydride and (b) y = 0.22 hydride. Arrott plots of (c) $La_{0.7}Ce_{0.3}Fe_{11.5-x}Mn_xSi_{1.5}$ and (d) $La_{0.7}Ce_{0.3}Fe_{11.55-y}Mn_ySi_{1.45}$ hydrides. The inset of Fig. 4(c) shows the DSC curves of x = 0.26 hydride. (e) The temperature dependence of the exponent n under a maximum field of 2 T for x = 0.26 hydride.

Fig. 5. (a) The T_C as a function of Mn content for $La_{0.7}Ce_{0.3}Fe_{11.55-y}Mn_ySi_{1.45}$

compounds and their hydrides. (b) The lattice constant and average Fe-Fe distance as a function of Mn content for $La_{0.7}Ce_{0.3}Fe_{11.55-y}Mn_ySi_{1.45}$ compounds and their hydrides.

Fig. 6. Temperature dependence of $-\Delta S_M$ for $La_{0.7}Ce_{0.3}Fe_{11.5-x}Mn_xSi_{1.5}$ and $La_{0.7}Ce_{0.3}Fe_{11.55-y}Mn_ySi_{1.45}$ hydrides under the magnetic field change of 0−1 T. The inset shows the maximum $-\Delta S_M$ value as a function of Mn content.

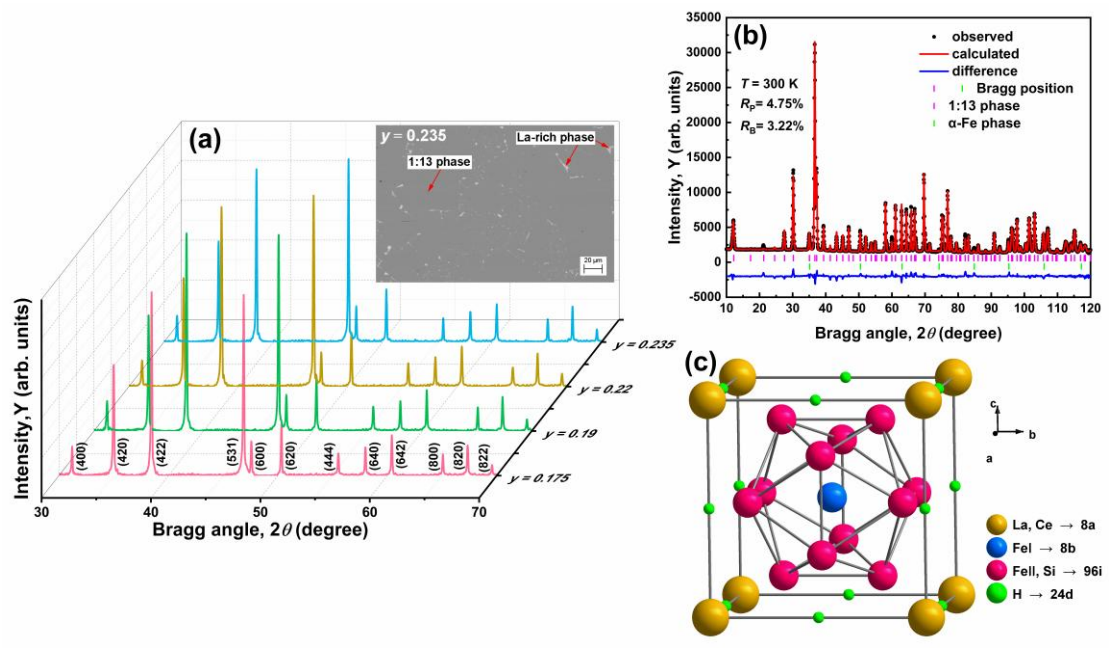

Fig. 1. (a) The powder XRD patterns of $La_{0.7}Ce_{0.3}Fe_{11.55-y}Mn_ySi_{1.45}$ (y = 0.175, 0.19, 0.22, 0.235) compounds at room temperature. The inset shows the backscattered SEM micrograph of y = 0.235 compound. (b) Neutron powder diffraction patterns of $La_{0.7}Ce_{0.3}Fe_{11.28}Mn_{0.22}Si_{1.5}$ hydride at 300 K. (c) Schematic structure of the 1/8 part of a cubic unit cell for $La(Fe,Si)_{13}$-based compounds.

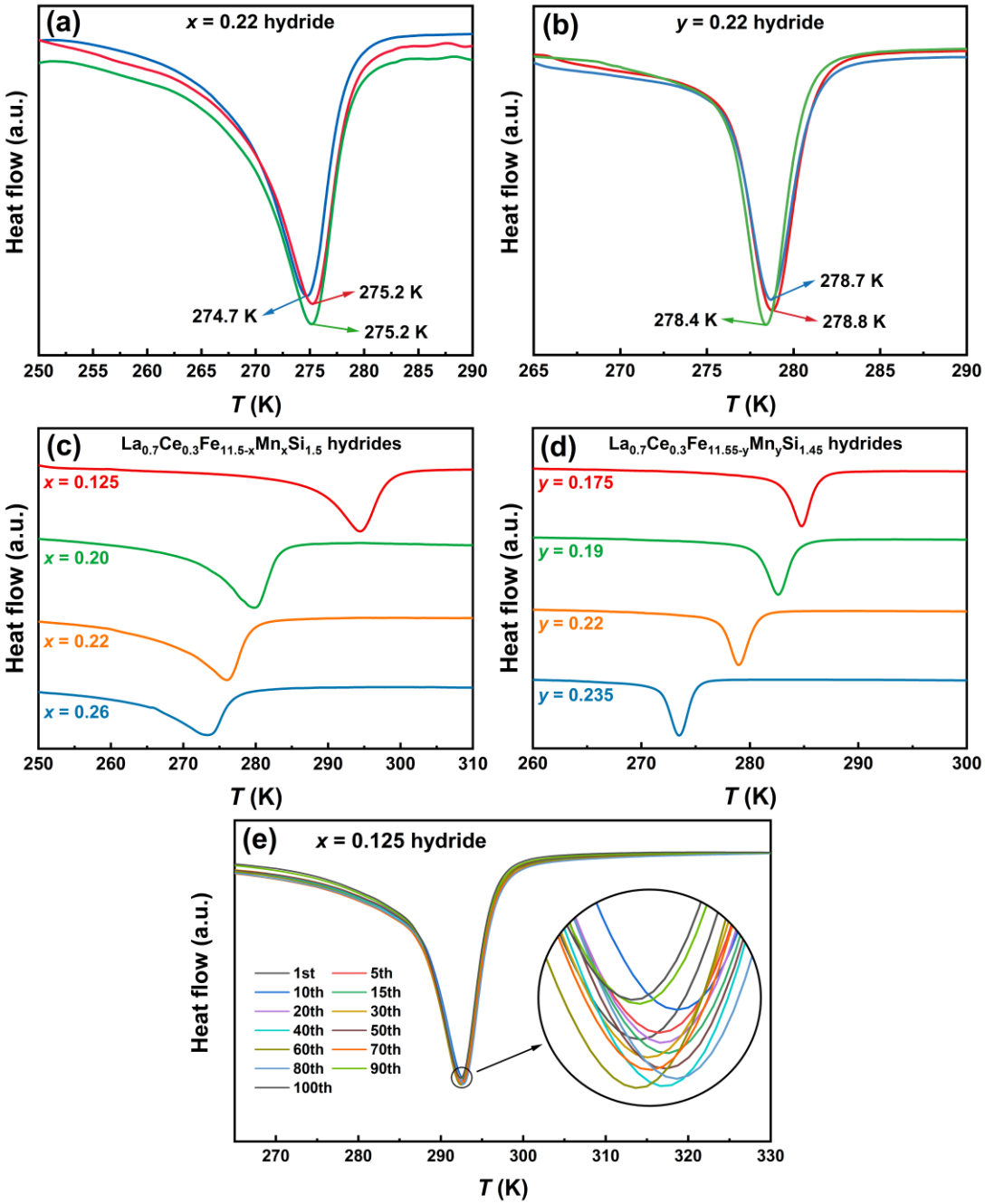

Fig. 2. DSC curves of three samples for (a) $La_{0.7}Ce_{0.3}Fe_{11.28}Mn_{0.22}Si_{1.5}$ hydride and (b) $La_{0.7}Ce_{0.3}Fe_{11.33}Mn_{0.22}Si_{1.45}$ hydride. The DSC curves during heating for (c) $La_{0.7}Ce_{0.3}Fe_{11.5-x}Mn_xSi_{1.5}$ hydrides and (d) $La_{0.7}Ce_{0.3}Fe_{11.55-y}Mn_ySi_{1.45}$ hydrides. (e) DSC curves of x = 0.125 hydride at the selected transition cycles.

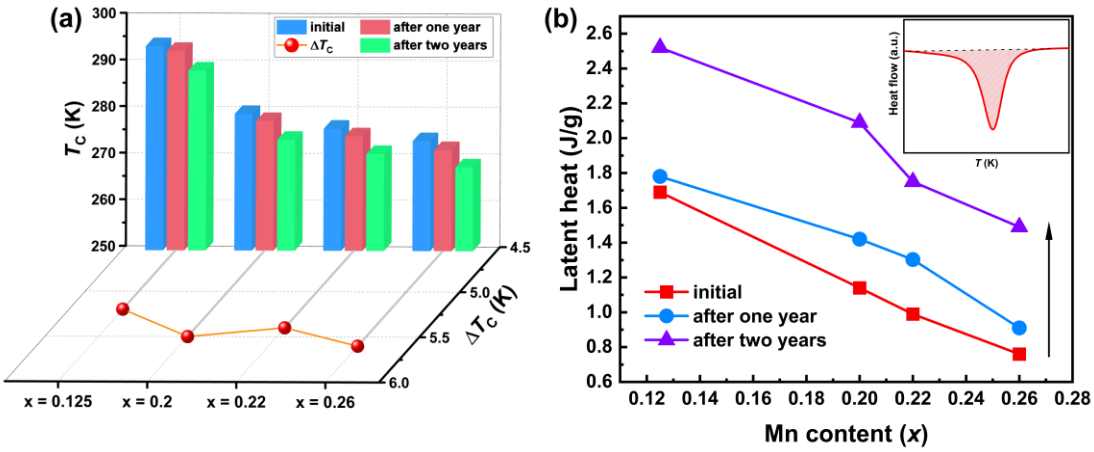

Fig. 3. (a) The T_C of the $La_{0.7}Ce_{0.3}Fe_{11.5-x}Mn_xSi_{1.5}$ hydrides measured after initial preparation, after one year, and after two years when held at room temperature and the ΔT_C between the initially-prepared samples and the samples held at room temperature for two years for $La_{0.7}Ce_{0.3}Fe_{11.5-x}Mn_xSi_{1.5}$ hydrides. (b) The latent heat as a function of Mn content for $La_{0.7}Ce_{0.3}Fe_{11.5-x}Mn_xSi_{1.5}$ hydrides held at room temperature for different time. The inset shows the schematic illustration of latent heat calculation.

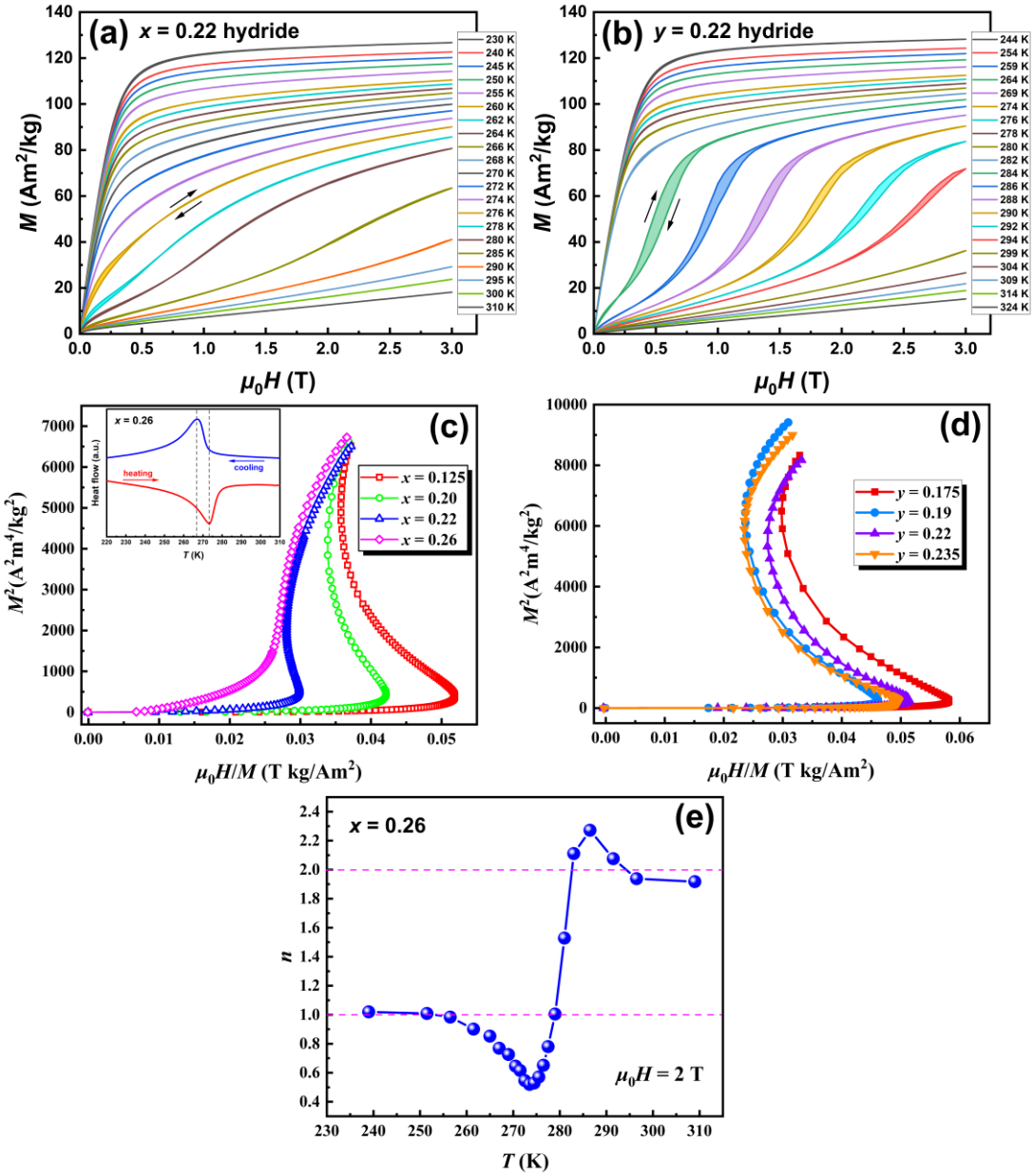

Fig. 4. Magnetization isotherms with magnetizing and demagnetizing processes for (a) x = 0.22 hydride and (b) y = 0.22 hydride. Arrott plots of (c) $La_{0.7}Ce_{0.3}Fe_{11.5-x}Mn_xSi_{1.5}$ and (d) $La_{0.7}Ce_{0.3}Fe_{11.55-y}Mn_ySi_{1.45}$ hydrides. The inset of Fig. 4(c) shows the DSC curves of x = 0.26 hydride. (e) The temperature dependence of the exponent n under a maximum field of 2 T for x = 0.26 hydride.

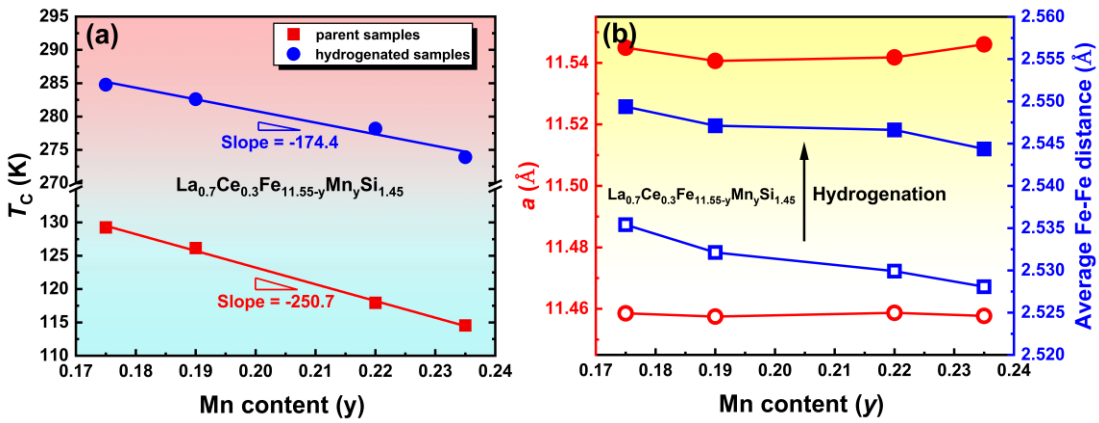

Fig. 5. (a) The T_C as a function of Mn content for $La_{0.7}Ce_{0.3}Fe_{11.55-y}Mn_ySi_{1.45}$ compounds and their hydrides. (b) The lattice constant and average Fe-Fe distance as a function of Mn content for $La_{0.7}Ce_{0.3}Fe_{11.55-y}Mn_ySi_{1.45}$ compounds and their hydrides.

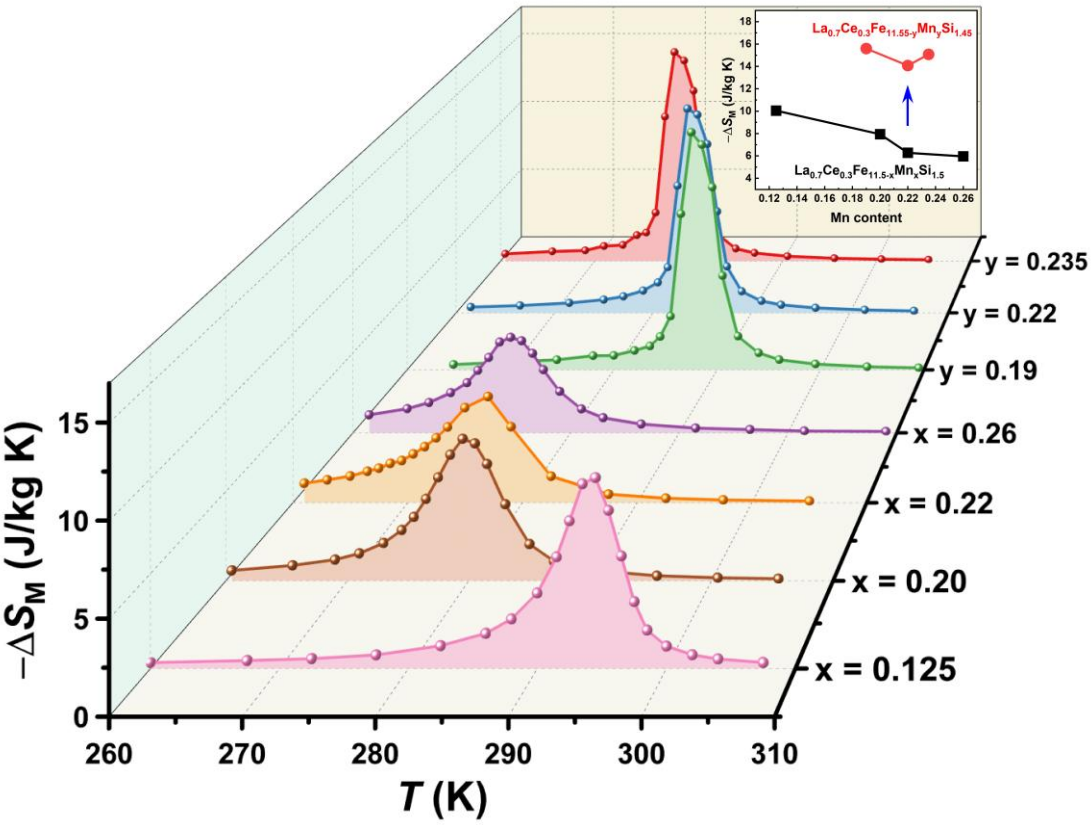

Fig. 6. Temperature dependence of $-\Delta S_M$ for $La_{0.7}Ce_{0.3}Fe_{11.5-x}Mn_xSi_{1.5}$ and $La_{0.7}Ce_{0.3}Fe_{11.55-y}Mn_ySi_{1.45}$ hydrides under the magnetic field change of 0−1 T. The inset shows the maximum $-\Delta S_M$ value as a function of Mn content.